



**Environmental
Science**
Processes & Impacts

**Impact of Bromide Exposure on Natural Organochlorine
Loss from Coastal Wetland Soils in the Winyah Bay, South
Carolina**

Journal:	<i>Environmental Science: Processes & Impacts</i>
Manuscript ID	EM-ART-12-2019-000604.R1
Article Type:	Paper

SCHOLARONE™
Manuscripts

1
2
3 1 The fate of naturally occurring organochlorine (org-Cl) compounds has become increasingly
4
5 2 important as we gain more insight into their role in contributing to detrimental environmental
6
7 3 impacts. Org-Cl compounds are persistent organic pollutants which can bioaccumulate and
8
9 4 contribute to ecosystem and human toxicity. Further, org-Cl compounds emitted to the
10
11 5 atmosphere undergo photolysis, producing chlorine radicals which catalytically destroy ozone. In
12
13 6 this study we show that bromination of organic carbon as salt-water intrudes into coastal
14
15 7 wetlands results in ubiquitous loss of org-Cl, most likely to the gaseous phase, allowing for
16
17 8 further perpetuation of ozone depletion and subsequent sea level rise. Our research underscores
18
19 9 the importance of halogen reactions in coastal ecosystems on global cycling of org-Cl and
20
21
22 10 ultimately on climate change.
23
24
25
26
27
28
29
30
31
32
33
34
35
36
37
38
39
40
41
42
43
44
45
46
47
48
49
50
51
52
53
54
55
56
57
58
59
60

1
2
3 1 **Impact of Bromide Exposure on Natural Organochlorine Loss from Coastal Wetland Soils**
4
5 2
6 **in the Winyah Bay, South Carolina**

7
8 3 Danielle R. Schlesinger, Satish C. B. Myneni

9
10 4 Department of Geosciences, Princeton University, Princeton, NJ 08544, USA.
11
12 5
13 6
14 7

15
16
17 7 **Abstract**
18

19 8 Naturally formed halogenated organic compounds are common in terrestrial and marine
20
21 9 environments and play an important role in the halogen cycle. Among these halogenated
22
23 10 compounds, chlorinated organic compounds are the most common halogenated species in all soils
24
25 11 and freshwater sediments. This study evaluated how a previously observed phenomenon of
26
27 12 bromination of organic matter in coastal soils due to salt-water intrusion impacts the stability and
28
29 13 fate of natural organochlorine (org-Cl) in coastal wetland soils. The reacted solid and liquid
30
31 14 samples were analyzed using X-ray spectroscopy (in cm and at micron scales for solids) and ion
32
33 15 chromatography. We find that introduction of Br⁻ species and their subsequent reactions with
34
35 16 organic carbon are associated with an average of 39% loss of org-Cl species from leaf litter and
36
37 17 soil. The losses are more prominent in org-Cl hotspots of leaf litter, and both aliphatic and aromatic
38
39 18 organochlorine compounds are lost from all samples at high Br⁻ concentrations. The combination
40
41 19 of solid and aqueous phase analysis suggests that org-Cl loss is most likely largely associated with
42
43 20 volatilization of org-Cl. Release of labile org-Cl compounds has detrimental environmental
44
45 21 implications for both ecosystem toxicity, and stratospheric ozone. The reactions similar to those
46
47 22 observed here can also have implications for the reactions of xenobiotic chlorinated compounds in
48
49 23 soils.
50
51
52
53
54
55
56
57
58
59
60

24

I.0 Introduction:

26 Natural organochlorine (org-Cl) compounds occur ubiquitously in soils and sediments, where they
27 form and accumulate as a result of organic matter decomposition¹. Many studies have reported
28 that these compounds occur in the concentration range of a few hundred to a few thousand mg/kg
29 (ppm) depending on the biogeochemistry of the local environment.²⁻³ In each of these studies, org-
30 Cl compounds were reported from diverse ecosystems, including soils², marine and estuarine
31 sediments⁴, peat bogs^{5,3}, and coniferous forests⁶.

33 The mechanisms of natural org-Cl compound formation have been examined, and these studies
34 have shown that chloride (Cl⁻) in soils and leaf litter can be converted to org-Cl through a variety
35 of pathways. These mechanisms may be biotic, where haloperoxidase enzymes produced by a
36 variety of microbial and fungal communities present in soil are used,^{7,8} or abiotic, where iron-
37 catalyzed oxidation of organic matter or halides are key reactants.⁹ Once produced, these natural
38 org-Cl compounds accumulate in soils and sediments over time because of the increased stability
39 from strong C-Cl bonds.

40

41 The biological toxicity and environmental impact (other than their role in the halogen cycle) of
42 these natural org-Cl compounds are unknown. However, many known anthropogenic org-Cl
43 compounds, such as poly-chlorinated biphenyls, for example, are highly toxic because of their high
44 stability and lipophilicity and are known to bioaccumulate in humans and cause detrimental health
45 effects, including hormone and endocrine system disruption and acute reproductive cancers.¹⁰⁻¹²
46 In addition to org-Cl toxicity, small org-Cl compounds, such as chloroform (CHCl₃), methyl

1
2
3 47 chloride (CH_3Cl), and a variety of other very short-lived substances (generally a few months
4
5 48 lifetime in the atmosphere), can volatilize from terrestrial systems, enter the atmosphere, and
6
7 49 undergo photolysis producing Cl radicals which react with and destroy stratospheric ozone.^{13,14}
8
9
10 50 For these reasons, transport, reactivity, and fate of naturally occurring org-Cl species and the
11
12 51 biogeochemical variables that control their behavior are of particular interest and concern.
13
14
15 52

16
17 53 This study on natural org-Cl associated with leaf litter and soil showed a surprising result and
18
19 54 indicated that these compounds are unstable in the presence of elevated levels of common
20
21 55 nucleophiles, such as bromide (Br^-). Due to recent trends in global warming and associated sea-
22
23 56 level rise in coastal systems, freshwater wetlands and their soil organic carbon are exposed to
24
25
26 57 elevated levels of Br^- , along with changes in other natural conditions, such as pH and elevated
27
28 58 concentration of other ions present in seawater. While each of these variables may influence the
29
30
31 59 stability of natural org-Cl compounds present in coastal wetlands of the Winyah Bay (SC)¹⁵, we
32
33 60 have previously observed that rise in sea level in this region has resulted in rapid, pervasive, and
34
35 61 preferential bromination of organic matter as freshwater wetlands are converted to salt-affected
36
37 62 wetlands.¹⁵ Because Br^- appears to be the key reactant in these coastal conditions, for this study,
38
39
40 63 we explored the exposure of Br^- on the natural org-Cl present in freshwater wetlands as they
41
42 64 undergo salination as a first step in understanding the complex reactions that may occur in these
43
44 65 ecosystems and impact overall Cl biogeochemistry and cycling. The findings from this study have
45
46
47 66 implications for the stability and fate of both natural and anthropogenic halogenated organic
48
49 67 compounds.
50

51 68

54 69 **II.0 Methods:**

55
56
57
58
59
60

70 ***II.1 Selection of Field Site and Sample Collection:***

71 The Winyah Bay, South Carolina is a coastal region in southeastern United States adjacent to the
72 Atlantic Ocean which has been well monitored and has experienced significant sea-level rise in
73 the past few decades.¹⁶ The Winyah Bay area has a humid, subtropical mid-latitude climate with
74 equally spread precipitation throughout the year including mid-latitude cyclones through the
75 winter months and convective thunderstorms during the summer months.¹⁷ Annual temperatures
76 vary between an average high of 25°C to low of 16°C.¹⁸ The coastal region contains wetlands
77 occurring across a salinity gradient from salt marsh, at highest salinity, to salt-affected wetland,
78 and to freshwater wetland, lowest salinity. For this study, leaf litter and soil samples were collected
79 only from the freshwater wetlands, which have not been exposed to seawater. The salinity in the
80 freshwater wetland is 0.25 (\pm 0.06) ppt (parts per thousand) throughout the year.¹⁵ The freshwater
81 wetland is forested with dominate tree species of bald cypress (*Taxodium disticum*), water tupelo
82 (*Nyssa aquatic*), and swamp tupelo (*Nyssa sylvatica* var. *biflora*). Samples were collected once in
83 three sections from a small area: leaf litter, 0-10 cm, and 10-20 cm. The samples were transferred
84 to Ziploc bags, sealed, and shipped on ice to Princeton, New Jersey, where they were stored in a
85 cold room in order to sustain the natural conditions prior to incubations with Br.

87 ***II. 2 Soil incubations with Br:***

88 Soil and leaf litter incubations were conducted in aerobic conditions (open to exchange with
89 atmospheric oxygen) intended to mimic aerobic and fluctuating hydrological conditions and the
90 transition of freshwater wetlands to salt-affected wetlands. This is in contrast to the salt marsh
91 conditions, which are considered to be relatively anoxic due to their being consistently submerged
92 with seawater. Additionally, the salt-affected wetland, oxic conditions were previously shown to

1
2
3 93 have the highest rate of bromination, likely due to increased organic carbon content and exposure
4
5 94 to oxygen.¹⁵ Leaf litter and soils in their natural state were reacted with Br⁻ (prepared as a solution
6
7 95 from KBr_(s)) of varying concentrations (0.1, 0.5, 1.0, and 3.0 mM). The concentration of Br⁻ in
8
9 96 seawater is ~0.8 mM, and the selected Br⁻ concentrations represent different amounts of either
10
11 97 dilution with freshwater or concentration of salinity.¹⁹ Concentrations of Br⁻ above those found in
12
13 98 seawater, and explored in this study, can potentially occur in conditions such as significant
14
15 99 evaporation of seawater from an isolated area inundated with seawater or presence of specific types
16
17 100 of vegetation that concentrate salt into their root systems. Further, this range of Br⁻ concentrations
18
19 101 creates a spectrum in which to explore the extent of bromination in end-case scenarios. Samples
20
21 102 without any externally added Br⁻ (0.0 mM) are ‘controls’, and these samples went through wet-dry
22
23 103 cycles with additions of just deionized milliQ water. For each incubation, 5 grams of soil were
24
25 104 reacted with 7.5 mL of Br⁻ solution at room temperature over the course of 12 days by 6 additions
26
27 105 of 1.25 mL of solution every other day. This Br⁻ addition scheme was intended to create a wetting
28
29 106 and drying cycle similar to natural tidal patterns observed in the coastal wetland system. The
30
31 107 incubations were open to the atmosphere throughout the 12-day period to allow for natural oxygen
32
33 108 exchange. Following the 12-day incubation, samples were thoroughly mixed to reduce
34
35 109 heterogeneity and washed with deionized milliQ water in order to remove excess unreacted salt
36
37 110 and prepare them for speciation analysis. A flow chart of sample phases and the methods used to
38
39 111 analyze them, described in the following paragraphs, is shown in Fig. S1.
40
41
42
43
44
45
46
47
48

49 113 *II. 3 Cl & Br speciation in soils & leaf litter:*

50
51 114 Speciation of Cl was conducted using X-ray absorption spectroscopy (XAS) at the Cl absorption
52
53 115 edge, and this was conducted at two different spatial scales: centimeter scale (2.5x0.2 cm²) to
54
55
56
57
58
59
60

1
2
3 116 evaluate the bulk, or average, Cl speciation in samples, and at the micron (1-15 μm^2) scale to
4
5 117 evaluate the possible heterogeneity in Cl speciation in individual particles.
6
7

8 118
9

10 119 ***II.3a Speciation at the centimeter scale:***

11
12 120 Samples were analyzed in their natural state without further preparation, *in-situ*, by sealing a thin
13
14 121 layer of the sample (about $\frac{1}{4}$ cm thick) between X-ray clean polyfilm and kapton tape before
15
16 122 placing in a He-filled X-ray chamber for spectral collection. The He-environment was used in the
17
18 123 sample chamber to both improve the detection of Cl fluorescence signal and to reduce the
19
20 124 probability of forming reactive oxygen species throughout X-ray exposure to the sample during
21
22 125 the approximately 20 min x-ray scan. All wet, soil and leaf litter samples were analyzed for bulk
23
24 126 Cl speciation on beamline 4-3 at the Stanford Synchrotron Radiation Light Source (SSRL). The
25
26 127 Cl K-edge XANES spectra were collected using a Vortex fluorescence detector with an energy
27
28 128 step size of 0.08 eV close to the Cl edge. The beam size was 1 x 0.1 cm^2 and the sampled area was
29
30 129 1.414 x 0.1 cm^2 . Chlorophenol red was used as a standard to calibrate the Cl absorption edge, with
31
32 130 the Cl 1s absorption maximum of the C-Cl aromatic bond set at 2821.1 eV. Spectra were
33
34 131 normalized using Demeter Athena²⁰ by fitting a first-order polynomial to the pre-edge region and
35
36 132 normalizing the post-edge region to 1.0 by fitting a first- or second-order polynomial depending
37
38 133 on the spectral shape. The Cl XANES spectra of structurally known model inorganic and organic
39
40 134 compounds were used to fit sample spectra using a linear combination fitting (LCF) procedure in
41
42 135 order to determine Cl valence state and coordination environment in each sample. These standard
43
44 136 spectra are: chlorophenol red (org-Cl_{arom}), chlorodecane (org-Cl_{ali}), glycine H-Cl (H-bonded inorg-
45
46 137 Cl), and NaCl_(aq) (hydrated inorg-Cl) (Fig. 1A). Fitting was done using these four standards, as
47
48 138 they are indicative of typical Cl bonding and are easily differentiated due to their energy shift
49
50
51
52
53
54
55
56
57
58
59
60

1
2
3 139 depending on Cl speciation. This analysis followed previous studies utilizing Cl K-edge XANES
4
5 140 to determine Cl speciation in soil and leaf litter samples.^{2,4,21} Some soil samples were also analyzed
6
7 141 on beamline 14-3 at SSRL (using a de-focused beam) and an energy step size of 0.15 eV close to
8
9 142 the Cl edge. In addition to Cl, cm-scale XANES were performed at the Br K-edge as part of a
10
11 143 previously published study with the same sample set up, and results showing production of org-Br
12
13 144 species after reaction are presented in that study.¹⁵
14
15
16
17 145

18
19 146 The relative abundances of Cl in wet samples was determined using the intensity of edge-step,
20
21 147 ~40-50 eV above the absorption edge of the background-corrected and unnormalized XANES
22
23 148 spectra.
24
25

26 149

27 28 150 *II.3b Speciation at the micron scale:*

29
30
31 151 High-resolution elemental maps of weathered bald-cypress leaf litter were made using
32
33 152 spectromicroscopic techniques in order to assess the heterogeneity in Cl speciation at the micron-
34
35 153 scale. Leaf samples were washed with deionized milliQ water to remove excess salt adsorbed to
36
37 154 the surface and mounted on plastic sample holders using XRF Tape TF-500 which is both halogen
38
39 155 and sulfur free (Fig. S2) backing and imaged at different energies (redox maps) close to the Cl K-
40
41 156 edge corresponding to the energy shifts determined by Cl standards. Org-Cl (chlorophenol red)
42
43 157 was run as a standard to determine the peak position of org-Cl_{arom}, from which the org-Cl_{ali} and
44
45 158 inorg-Cl edge energies could be determined based on known energy shifts of standards discussed
46
47 159 above. These energies were 2820.5 eV (org-Cl_{ali}), 2821.1 eV (org-Cl_{arom}), and 2823.1 eV (inorg-
48
49 160 Cl), and are shown with arrows in Fig. 1A. A higher energy map was also collected at 2900 eV to
50
51
52 161 observe total Cl abundance. After initial imaging, the mounted leaves were reacted with 1 mL of
53
54
55
56
57
58
59
60

1
2
3 162 0.1 mM Br⁻ solution (as a thin-film of solution on the surface of the leaf).¹⁹ Excess solution was
4
5 163 siphoned off after approximately 2-3 hours, and the samples were allowed to air dry for an
6
7 164 additional 3-4 hours. The leaves were washed with deionized milliQ water to remove excess
8
9 165 soluble salts from the leaf surface and re-imaged at the exact same locations and energies to
10
11 166 examine speciation variations after the reaction. Micro-XANES (μ -XANES) spectra for Cl were
12
13 167 collected at Cl hotspots (high Cl fluorescence intensity) both before and after the reaction in the
14
15 168 same locations.
16
17
18
19 169

20
21 170 In addition to Cl, Br speciation maps were simultaneously collected at the same locations and with
22
23 171 the same parameters as with Cl maps in order to observe Br speciation in leaf litter and correlation
24
25 172 with Cl. Br redox maps were collected at 13473.0 eV (org-Br), 13476.0 eV (inorg-Br), and 13500
26
27 173 eV (high energy). Only one energy was selected for org-Br because the intense x-ray absorption
28
29 174 features for org-Br_{ali} and org-Br_{arom} are too close to differentiate from one another (Fig. S6A). A
30
31 175 set of Br μ -XANES was also collected from Br hotspots in the same locations before and after
32
33 176 reaction. Aqueous potassium bromide (KBr) was used as a standard to calibrate the Br absorption
34
35 177 edge, with the Br 1s absorption maximum set at 13476.0 eV.
36
37
38
39 178

40
41 179 One set of Cl maps was collected on beamline 14-3 at SSRL under a He environment using a
42
43 180 vortex detector with a 15-micron step size. Br maps were also collected at beamline 5-ID (SRX)
44
45 181 at the National Synchrotron Radiation Lightsource II with a 1-micron step size. All other sets of
46
47 182 leaf litter Cl and Br maps were collected on GSECARS beamline 13-IDE at the Advanced Photon
48
49 183 Source (APS) under a He atmosphere. The maps and μ -XANES spectra were collected using a
50
51 184 vortex ME4 silicon drift diode array detector. Maps were collected with a 10-micron step size, and
52
53
54
55
56
57
58
59
60

1
2
3 185 μ -XANES for both Cl and Br were collected with a 0.2 eV step size around the Cl or Br edge,
4
5 186 respectively.

6
7 187
8
9
10 188 All images were first normalized to the incident photon counts, and analyzed using Sam's
11
12 189 Microprobe Analysis Kit (SMAK)²² and Larch: Data Analysis Tools for X-Ray Spectroscopy.²³
13
14 190 The Larch software was also used to determine total Cl and Br fluorescence intensity (counts per
15
16
17 191 second, cps) of leaf litter hotspots, intermediate spots, and background spots. The μ -XANES
18
19 192 spectra for both Cl and Br were analyzed using Athena as previously described for the XANES
20
21
22 193 spectral analysis of bulk soil and leaf litter samples.

23
24 194

25 26 195 *II.4 Estimating Cl abundances in solid samples using X-ray Fluorescence (XRF):*

27
28 196 The concentration of total Cl (inorg-Cl + org-Cl) in incubated and dried soil samples was measured
29
30
31 197 using XRF analysis. Each sample, including controls, was washed thoroughly with 25 mL of
32
33 198 deionized milliQ water to remove excess soluble halides. Following washing, each sample was
34
35 199 dried overnight in an oven at 50°C and then ground to a fine powder using a diamonite mortar and
36
37
38 200 pestle. From each sample 3-5 9mm pellets were made using a hydraulic press by applying 5 tons
39
40 201 of pressure for 2 minutes. Each pellet was placed between a polycarbonate disk and X-ray clean
41
42 202 polyfilm and examined using a Rigaku Supermini200 wavelength dispersive XRF Spectrometer
43
44
45 203 under vacuum. An RX25 monochromator crystal and a scintillation counter were used to detect
46
47 204 Cl. For each of the three sample depths (leaf litter, 0-10 cm, and 10-20 cm), a set of Cl standards
48
49 205 was created by standard addition of KCl solution in increasing concentrations (0-200 ppm) to
50
51
52 206 create a standard curve. These standard curves were used to estimate the concentration of Cl in
53
54 207 each sample. In addition to Cl, XRF was performed to analyze total Br concentration as part of a

1
2
3 208 previously published study with the same sample set up, and results showing increased total Br
4
5 209 after reaction are presented in that study.¹⁵
6
7

8 210

9
10 211 ***II.5 Aqueous phase Cl⁻ analysis with Ion Chromatography (IC) and XANES:***
11

12 212 All reacted soil and leaf litter samples were washed with 25 mL of deionized milliQ water to
13
14 213 remove any water-soluble Cl⁻ and other Cl species that may have formed during the course of the
15
16
17 214 reaction. The collected solution was filtered using a 0.2 µm syringe filter to remove all suspended
18
19 215 solids. All sample filtrates were analyzed for Cl⁻ concentration on a Dionex ion chromatography
20
21 216 system equipped with an IC25 Ion Chromatograph, AS40 autosampler, an LC25 chromatography
22
23
24 217 oven and an EG40 eluent generator. Anions were separated using a Dionex IonPac AS15 (3 × 150
25
26 218 mm) analytical column connected to a Dionex IonPac AG15 (3 × 50 mm) guard column. A set of
27
28 219 Cl⁻ standards with varying Cl concentrations was run and used to calculate the Cl concentrations
29
30
31 220 of samples. The output from the IC analysis determined concentration of Cl⁻ in the aqueous phase
32
33 221 on a mg/L basis. This value was then converted to total amount of mg Cl⁻/kg soil lost from each
34
35 222 sample using the total amount of water (25 mL) with which each sample was washed and the total
36
37 223 amount of reacted soil per sample (0.005 kg). The collected aqueous portions from leaf litter and
38
39 224 soil reactions were further analyzed by XANES in order to determine Cl speciation in aqueous and
40
41 225 particulate organic matter phases. Because the Cl concentration is too low in the water extracts for
42
43 226 Cl XANES analysis, the filtrates (used for IC) were dried onto a halogen-free tape surface as a thin
44
45 227 film to study with XANES spectroscopy. Unfiltered sample solutions were filtered through P5
46
47 228 grade filter paper, and the particulate organic matter was collected on the filter paper and allowed
48
49 229 to dry. Both the thin-film filtrates and particulate organic matter were analyzed for Cl speciation
50
51
52 230 on beamline 13-IDE at the APS by Cl K-edge XANES as previously described.
53
54
55
56
57
58
59
60

1
2
3 2314
5 232 **III.0 Results and Discussion:**6
7 2338
9 234 ***III.1 In-situ Cl speciation of bulk soil and leaf litter***10 235 The in-situ, wet XANES analyses of the bulk leaf litter and soil samples not exposed to Br⁻ show11 236 a sharp and strong peak corresponding to org-Cl, while the Br⁻ reacted samples clearly show a loss12 237 in org-Cl signal at higher concentrations of added Br⁻ (Fig. 1). The org-Cl XANES spectra of

13 238 examined standards show a sharp, lower energy peak when compared with inorg-Cl XANES (Fig.

14 239 1A). In leaf litter and both examined soil depths, the Cl-XANES spectra of samples lose the

15 240 spectral features at low energy, and the spectra shift to higher energy progressively with increasing

16 241 Br⁻ concentration. The changes are pronounced at highest concentrations of Br⁻ added, which

17 242 indicates a change in speciation from org-Cl to largely inorg-Cl coordination. Unnormalized edge

18 243 step intensity in the XANES spectra, which is an indicator of relative total Cl abundance (inorg-

19 244 Cl + org-Cl), shows a greater than 50% loss in Cl signal in leaf litter (70 (± 3)%) and the 10-20 cm

20 245 soil depth (63 (± 3)%) (Fig. 2). The 0-10 cm depth (38 (± 3)%) also shows a similar trend in

21 246 intensity loss, but not as pronounced as the others. The average loss in total Cl fluorescence

22 247 intensity across all three depths is 57 (± 3) %. The percent error was calculated as a function of

23 248 variability in intensity changes between each sample in order to include variability that may arise

24 249 from variation in composition and preparation of samples. While samples for this analysis were

25 250 mounted as consistently as possible, absolute concentrations are difficult to estimate with high

26 251 accuracy in this wet *in-situ* analysis because of differences in sample packing, density and water

27 252 content, and thus these represent relative concentrations and relative error. The LCF analysis of

28 253 XANES spectra, which provides speciation information, shows both org-Cl_{ali} and org-Cl_{arom}

29

30

31

32

1
2
3 254 species are present initially in all samples, and both forms are lost at the highest concentration of
4
5 255 added Br⁻ concentration (3.0 mM) (Table 1, Table S1). At lower concentrations of added Br⁻ in
6
7 256 some samples, the org-Cl spectral character actually increases, for example from 0 to 1.0 mM Br⁻
8
9
10 257 . This is most likely a result of sample heterogeneity, and while the org-Cl spectral character may
11
12 258 increase, the total Cl content decreases simultaneously as is observed by the unnormalized edge-
13
14 259 step intensity. The LCF overall shows an average of 39% loss in org-Cl spectral character,
15
16 260 corresponding to loss in total org-Cl compounds (Cl_{ali} + Cl_{arom}). Based on in-situ XANES analysis
17
18 261 of wet samples, addition of Br⁻ results in overall loss in total Cl abundance, but more significantly,
19
20 262 a substantial loss of org-Cl compounds present in soil or leaf litter.
21
22
23
24 263

26 264 ***III.2 Spectromicroscopy of Cl and Br in leaf litter***

28 265 Because the bulk, wet, in-situ XANES analysis of leaf litter showed the most dramatic loss in org-
29
30 266 Cl upon exposure to Br⁻, these samples were analyzed further at the micron-scale in order to assess
31
32 267 the heterogeneity in Cl speciation and reactivity throughout the sample. Heterogeneity in both
33
34 268 location and speciation of Cl hotspots may be dependent on a variety of variables, but are likely
35
36 269 mainly dependent on mechanisms of chlorination, such as biotic versus abiotic. For example, those
37
38 270 produced through enzymatic processes might be found in proximity to fungal structures in soil or
39
40 271 leaf litter, and their speciation may generally differ from those formed through abiotic
41
42 272 mechanisms.²⁴ Maps of degraded leaf litter imaged before and after reaction with dilute Br⁻
43
44 273 solution (0.1 mM; ~10% of Br⁻ in seawater) show a loss of Cl fluorescence intensity in all parts of
45
46 274 the leaf (Fig. 3). Cl containing regions in the maps were separated into 3 categories based on Cl
47
48 275 relative fluorescence intensity (counts per second, cps) in the org-Cl_{ali} map (Fig. 3A): hotspots
49
50 276 (>10,000 cps), intermediate spots (5,000-10,000 cps), and background spots <5,000 cps (Fig. 4).
51
52
53
54
55
56
57
58
59
60

1
2
3 277 The same intensity scales were used for Org-Cl_{arom} and inorg-Cl map analysis, however
4
5 278 fluorescence intensity ranges were shifted up by 5,000 cps and 10,000 cps, respectively. This
6
7
8 279 adjustment accounts for increased total Cl fluorescence intensity with increasing map energy,
9
10 280 which results from incorporation of all fluorescence from Cl species below that map's energy.
11
12 281 Hotspots and background spots are an average of 10 measured spots, and intermediate spots are
13
14
15 282 an average of 5 measured spots in each map.
16

17 283
18
19 284 The Cl-hotspots show a dramatic decrease in Cl fluorescence intensity (average loss 57%) after
20
21 285 reaction with Br⁻ for all Cl speciation types (inorg-Cl + org-Cl) (Fig. 4). Intermediate spots show
22
23 286 a small decrease in fluorescence intensity, while background spots show little to no change. The
24
25
26 287 Cl-hotspots show the greatest loss in total Cl and org-Cl fluorescence intensity after reaction,
27
28 288 suggesting that org-Cl loss is variable with respect to heterogeneity of leaf litter. Further, pervasive
29
30 289 loss of Cl fluorescence intensity in both org-Cl_{ali} and org-Cl_{arom} maps suggests that org-Cl loss is
31
32
33 290 not necessarily dependent on local coordination of org-Cl. Rather, both org-Cl_{ali} and org-Cl_{arom} can
34
35 291 be lost as a result of bromination of org-Cl containing organic matter.
36

37 292
38
39
40 293 The Cl hotspots were selected from the org-Cl maps (Fig. 3A) and were analyzed further in greater
41
42 294 detail for Cl-speciation variations by collecting μ -XANES spectra at these spots before and after
43
44
45 295 reaction with Br⁻. Before reaction, the Cl μ -XANES spectra were less noisy and showed sharp,
46
47 296 low energy org-Cl peaks (with the exception of spot 4, which has more inorganic-Cl) (Fig. S3A).
48
49 297 The peak intensities decreased in many of the spectra after reaction (nearly lost in some spots, such
50
51 298 as in spots 3 and 5; Fig. S3B). In addition, spectra collected after Br⁻ reaction are noisy, indicating
52
53
54 299 very low Cl signal or low Cl abundance. Analysis of the unnormalized edge-step for the μ -XANES
55
56
57
58
59
60

1
2
3 300 spectra from different spots before and after reaction showed 87% (\pm 3%; average) loss of Cl
4
5 301 fluorescence intensity (Fig S3C). This indicates a dramatic loss in relative total Cl abundance in
6
7 302 the leaf litter (inorg-Cl + org-Cl), and this is greater than the loss reported for the bulk analysis of
8
9 303 leaf litter, discussed above. The LCF of these spectra (Table S2) shows consistently high loss in
10
11 304 org-Cl_{ali} species, whose fraction drop to nearly zero in some of the μ -XANES spectra, and a
12
13 305 significant loss in org-Cl_{arom} character after reaction. This further indicates that org-Cl loss occurs
14
15 306 regardless of org-Cl bonding environment in leaf litter or soil. Overall, μ -XANES LCF shows a
16
17 307 combined loss of 47% of org-Cl character corresponding to loss in total org-Cl compounds (Cl_{ali}
18
19 308 + Cl_{arom}) in Br⁻ reacted leaf litter. This is consistent with observed loss in org-Cl from the leaf litter
20
21 309 bulk analysis reported above.
22
23
24
25
26
27
28

29 311 The leaf litter samples, described above, were also analyzed at the Br K-edge before and after
30
31 312 reaction in order to assess Br speciation at the micron-scale and its relationship with Cl species.
32
33 313 Br speciation maps show an increase in Br fluorescence intensity at both the org-Br and inorg-Br
34
35 314 edge energies (Fig. S4). As with the Cl maps, Br abundance in Br maps was also analyzed by
36
37 315 tracking changes of Br fluorescence intensity before and after reaction in Br hotspots (>50,000
38
39 316 cps), intermediate spots (10,000-50,000 cps), and background spots (<10,000 cps). Hotspots show
40
41 317 an overall increase in fluorescence intensity after reaction for all Br forms (average increase 65%)
42
43 318 (Fig. S5), which is relatively close to the observed loss in Cl fluorescence intensity (57%). The
44
45 319 locations (x,y coordinates) of Cl and Br hotspots can be compared qualitatively in order to assess
46
47 320 if org-Cl loss occurs exactly where bromination takes place. Maps showing changes in
48
49 321 fluorescence intensity for both org-Cl and org-Br are shown in Fig. 5. In these maps, spots of
50
51 322 highest org-Cl fluorescence intensity were determined by subtraction of org-Cl cps after reaction
52
53
54
55
56
57
58
59
60

1
2
3 323 from org-Cl cps before reaction. Similarly, spots of highest org-Br fluorescence intensity were
4
5 324 determined by subtraction of org-Br cps before reaction from org-Br cps after reaction. While there
6
7
8 325 is some overlap in the location of org-Cl and org-Br hotspots, the majority of org-Br spots do not
9
10 326 appear to correlate with instances of high org-Cl intensity before reaction. This simply suggests
11
12 327 that incorporation of Br species does not directly replace Cl in molecules. Because org-Cl loss
13
14 328 appears to occur heterogeneously with respect to the location of bromination, it is possible that
15
16
17 329 bromination of organic material destabilizes or degrades macromolecules containing org-Cl,
18
19 330 creating smaller species of org-Cl that can more easily partition to other phases, such as aqueous
20
21
22 331 or gaseous. Analysis of Br hotspots by μ -XANES (Fig. S6) shows both inorg-Br and org-Br species
23
24 332 to be present before and after reaction with Br⁻. The inorg-Br fraction appears to increase slightly
25
26 333 relative to org-Br species after reaction, which is likely due to adsorption of Br⁻ to the leaf surface
27
28
29 334 during the short reaction time (Table S3).

30
31 335

32 33 336 ***III.3 Ex-situ analysis of Cl abundances in soil and leaf litter***

34
35 337 To complement the *in-situ* synchrotron X-ray analysis, total Cl abundances (inorg-Cl + org-Cl) in
36
37
38 338 reacted soil and leaf litter samples were also estimated utilizing XRF (Fig. 6A). However, samples
39
40 339 for this measurement must be in a dry state. In both the leaf litter and soil samples from the 10-20
41
42 340 cm depth, Cl loss occurred on a similar scale of org-Cl loss observed in the wet *in-situ* bulk Cl-
43
44
45 341 XANES analysis (39%), but to a smaller extent than when compared with the total Cl loss observed
46
47 342 in the wet *in-situ* bulk analysis (57%). The 0-10 cm depth samples show relatively unchanging Cl
48
49 343 concentration with increasing added Br⁻, which is consistent with the variability observed for this
50
51 344 soil depth from the XANES analysis. While the XRF analysis shows some agreement with the *in-*

1
2
3 345 *situ* XANES analysis of bulk leaf litter and soil incubations in general, the XRF data is highly
4
5 346 variable with a calculated error of 20.5% total Cl.
6
7
8 347

9
10 348 The observed inconsistency and high analytical variability of XRF when compared to *in-situ*
11
12 349 XANES analysis may be due to artefacts associated with sample drying for XRF analysis. Recent
13
14 350 studies assessing the transport and precipitation of salts in soils have shown that salts become
15
16 351 increasingly concentrated in soil pore waters and are transported to the soil surface and precipitate
17
18 352 on the surface as evaporation and drying occurs.^{25,26} While the soils for XRF analysis were washed
19
20 353 prior to drying, differences in precipitation of trapped salts on the sample surface during drying
21
22 354 would lead to inaccurate and variable estimation of total Cl for XRF analysis. The X-ray
23
24 355 penetration depth at the Cl K-edge is on the scale of 1 micron, while the full sample is about ¼ of
25
26 356 a centimeter thick (the Br K-edge, for comparison, has a penetration depth of a few hundred
27
28 357 microns). For this reason, the dry XRF analysis is significantly affected by surface artefacts, rather
29
30 358 than the bulk composition of the sample. Further this surface transport and precipitations would
31
32 359 vary based on the inherent structural differences of porous media in soil (e.g. porosity, amount of
33
34 360 organic matter and amorphous materials that can retain hydrated ions). However, this surface
35
36 361 precipitation is not an issue for the *in-situ* XANES analysis of wet samples, as salts are less likely
37
38 362 to precipitate on the surface without drying, and strongly indicates that org-Cl is consistently lost
39
40 363 from the solid phase. Sample drying and analysis by XRF can lead to incorrect estimates of light
41
42 364 elements because of shallow X-ray penetration, and researchers should be cautious with the
43
44 365 interpretation of XRF results of dry porous materials.
45
46
47
48
49
50

51 366

52
53
54 367 ***III. 4 Aqueous phase analysis of Cl species***
55
56
57
58
59
60

1
2
3 368 Aqueous phase analysis of Cl^- , conducted using ion chromatography (IC), indicates that Cl^-
4
5 369 concentration did not change with Br^- exposure (Fig. 6B). In other words, the org-Cl lost from bulk
6
7 370 soil and leaf litter incubations was not dehalogenated, broken down, and released as Cl^- to the
8
9 371 aqueous phase. The average amount of Cl^- that is predicted to be in the aqueous phase of each
10
11 372 sample, assuming all the lost org-Cl species were completely broken down to Cl^- , was determined
12
13 373 in order to compare with the amount of Cl^- measured in the aqueous phase of each sample. The
14
15 374 percentages of total Cl abundance loss (inorg-Cl + org-Cl) observed from XANES analysis (70%
16
17 375 for leaf litter, 38% for 0-10 cm, and 63% for 10-20 cm) of bulk, reacted leaf litter and soil samples
18
19 376 were applied to the Cl concentration determined in the unreacted leaf and soil samples. This value
20
21 377 is the potential Cl^- concentration in the aqueous phase if all lost Cl was released as Cl^- (dashed
22
23 378 lines, Fig. 6B). In all samples, org-Cl lost as Cl^- is small. For all three depths in this study, the
24
25 379 released Cl^- is between 8.2-20.9 mg Cl^-/kg soil. For both the leaf litter and 10-20 cm depth, this
26
27 380 value is between 4-8% of the predicted total Cl loss. For 0-10 cm depth, the Cl^- concentration in
28
29 381 the filtrate only accounts for between 25-35% of predicted total Cl loss. These results suggest a
30
31 382 very small percentage of Cl species present in leaf litter or soil are completely dehalogenated and
32
33 383 lost as aqueous Cl^- species.
34
35
36
37
38
39

40 384
41
42 385 While the columns used in IC are sensitive to inorganic Cl^- , Cl-XANES spectroscopy was utilized
43
44 386 to determine the possible presence of org-Cl in filtrates and in particulate organic matter isolated
45
46 387 from the aqueous phase after reaction with Br^- . The Cl XANES of filtrates indicate that Cl is mostly
47
48 388 in the inorg-Cl form (Fig. S7A, Table S4). Speciation analysis of aqueous phase particulate organic
49
50 389 matter shows increased org-Cl character when compared to filtrates (Fig S7B, Table S4). The
51
52 390 particulate organic matter shows 20-50% org-Cl character in the XANES spectra, while the
53
54
55
56
57
58
59
60

1
2
3 391 aqueous filtrates did not show any org-Cl character in all samples except for one. However, the
4
5 392 low fluorescence intensity of the particulate organic matter spectra indicates that, while some org-
6
7 393 Cl is released into aqueous phase particulate organic matter, this portion is small compared with
8
9 394 the total org-Cl loss observed from the bulk reacted samples. These combined data predict that Cl
10
11 395 species may be volatilized and released to the gaseous phase.
12
13
14
15 396

16 17 397 **IV.0 Conclusions**

18
19 398 In summary, our studies show that org-Cl, the primary form of Cl in leaf litter and soils, is lost
20
21 399 upon exposure to Br⁻ containing aqueous solutions, and especially at higher concentrations of Br⁻,
22
23 400 and this loss varies with the amount of Br⁻ exposure, and the nature of the sample. In addition,
24
25 401 bromination of organic matter is concomitant with org-Cl loss, however, microscopy studies do
26
27 402 not suggest that they co-occur in the same regions and that both org-Cl_{ali} and org-Cl_{arom} speciations
28
29 403 can be lost. Among all the examined samples, leaf litter showed the highest org-Cl loss, suggesting
30
31 404 differences in org-Cl speciation in soils may be playing an important role in the reactions. The org-
32
33 405 Cl species present in leaf litter and soils may not be water soluble (as noticed from little loss of
34
35 406 org-Cl species when samples are washed/'reacted' with DI water), and this is likely because these
36
37 407 molecules are incorporated into larger insoluble macromolecules of natural organic matter.
38
39 408 However, additions of Br⁻ may be responsible for promoting the breakdown of the Cl containing
40
41 409 macromolecules, allowing them to be released from the solid phase. The reaction mechanisms
42
43 410 involving the breakdown of natural organohalogenes are unknown at this stage; however, these are
44
45 411 expected to be more complex when compared with smaller anthropogenic org-Cl compounds.²⁷
46
47 412 Some studies of org-Cl compounds in the natural environment have indicated that dechlorination
48
49 413 and dehalogenation reactions may occur readily, however they are mechanistically diverse and
50
51
52
53
54
55
56
57
58
59
60

1
2
3 414 dependent on local environmental conditions.²⁸ Many of these studies focus on biotic pathways in
4
5 415 the natural environment, while abiotic pathways are not well understood. Based on the results
6
7 416 presented in this study, we suggest that bromination of organic matter may influence subsequent
8
9 417 degradation of organic carbon and org-Cl containing organic matter present in leaf litter and
10
11 418 wetland soils. The absence of decay products, inorganic Cl⁻ and org-Cl, in the aqueous phase
12
13 419 suggest that Cl containing molecules are volatilized from the Br⁻ reacted soils during the reactions.
14
15 420 While the mechanisms for this process are unclear at this stage in the research, it is possible that
16
17 421 they follow natural biodegradation pathways associated with production of volatile org-Cl
18
19 422 compounds, and that reactivity of Br⁻ with soil organic carbon induces similar degradation
20
21 423 mechanisms and end results. Based on observed org-Cl loss, the abundances of gaseous chlorinated
22
23 424 compounds are expected to be in the range of parts per trillion. These measurements are difficult
24
25 425 to accomplish with typical gas chromatography instrumentation set ups due to the expected high
26
27 426 volatility and very low concentration, and will thus be explored with specialized equipment in
28
29 427 continuing work.
30
31
32
33
34
35
36

37 428
38 429 The results from this study point to the loss of natural org-Cl compounds, possibly as volatile org-
39
40 430 Cl molecules, in freshwater wetlands as soil organic carbon undergoes bromination, an emerging
41
42 431 phenomenon in coastal wetlands impacted by sea level rise. While there are a variety of variables
43
44 432 associated with sea-level rise that may influence overall fate of org-Cl compounds, this study
45
46 433 focused specifically on understanding the role of bromination on organic carbon and natural org-
47
48 434 Cl compounds as a first step in uncovering the complex and ongoing halogen chemistry occurring
49
50 435 in coastal ecosystems. Org-Cl compounds emitted into the atmosphere can photolyze, creating
51
52 436 chlorine radicals which catalytically destroy stratospheric ozone. A number of studies have shown
53
54
55
56
57
58
59
60

1
2
3 437 coastal wetlands and salt-marshes to be a major source of natural halocarbon emissions due to
4
5 438 seawater intrusion, and loss of org-Cl compounds and possible biogeochemical reactions in these
6
7 439 ecosystems may be similar to those observed in this study.^{29,30} As seawater intrusion into
8
9 440 freshwater ecosystems occurs more frequently in a changing climate, it is possible that volatile
10
11 441 org-Cl emissions will be further observed in areas not previously accounted for in org-Cl
12
13 442 biogeochemical cycling. In addition, the results of this study are of particular interest to the fate of
14
15 443 manmade org-Cl compounds, as they are considered to be persistent organic pollutants which can
16
17 444 bioaccumulate and contribute to ecosystem, animal, and human toxicity. Ultimately, these
18
19 445 reactions play an important role in the global cycling of org-Cl and their downstream influence on
20
21 446 ecosystem health and climate change.
22
23
24
25

26 447

27
28 **448 Acknowledgements:**

29
30 449 We thank Renxing Liang and the Onstott Group at the Department of Geosciences at Princeton
31
32 450 University for their assistance with and use of their Ion Chromatograph. This research is funded
33
34 451 by the National Science Foundation Graduate Research Fellowships Program (D.S), the National
35
36 452 Science Foundation Geobiology (grant # 1529956 to SM), and Chemical Sciences (grant #
37
38 453 1609927 to SM), The Phillips Equipment Fund from the Department of Geosciences at Princeton
39
40 454 University, and The Princeton Environmental Institute Walbridge Fund Graduate Award. We
41
42 455 would like to thank Dr. Chow at Clemson University for providing some of the samples examined
43
44 456 in this study. We thank the beamline scientists and staff from the Stanford Synchrotron Radiation
45
46 457 Lightsource, the Advanced Photon Source, and the National Synchrotron Radiation Lightsource II
47
48 458 for their help with the setting up of the stations. Use of the Stanford Synchrotron Radiation
49
50 459 Lightsource, SLAC National Accelerator Laboratory, is supported by the U.S. Department of
51
52
53
54
55
56
57
58
59
60

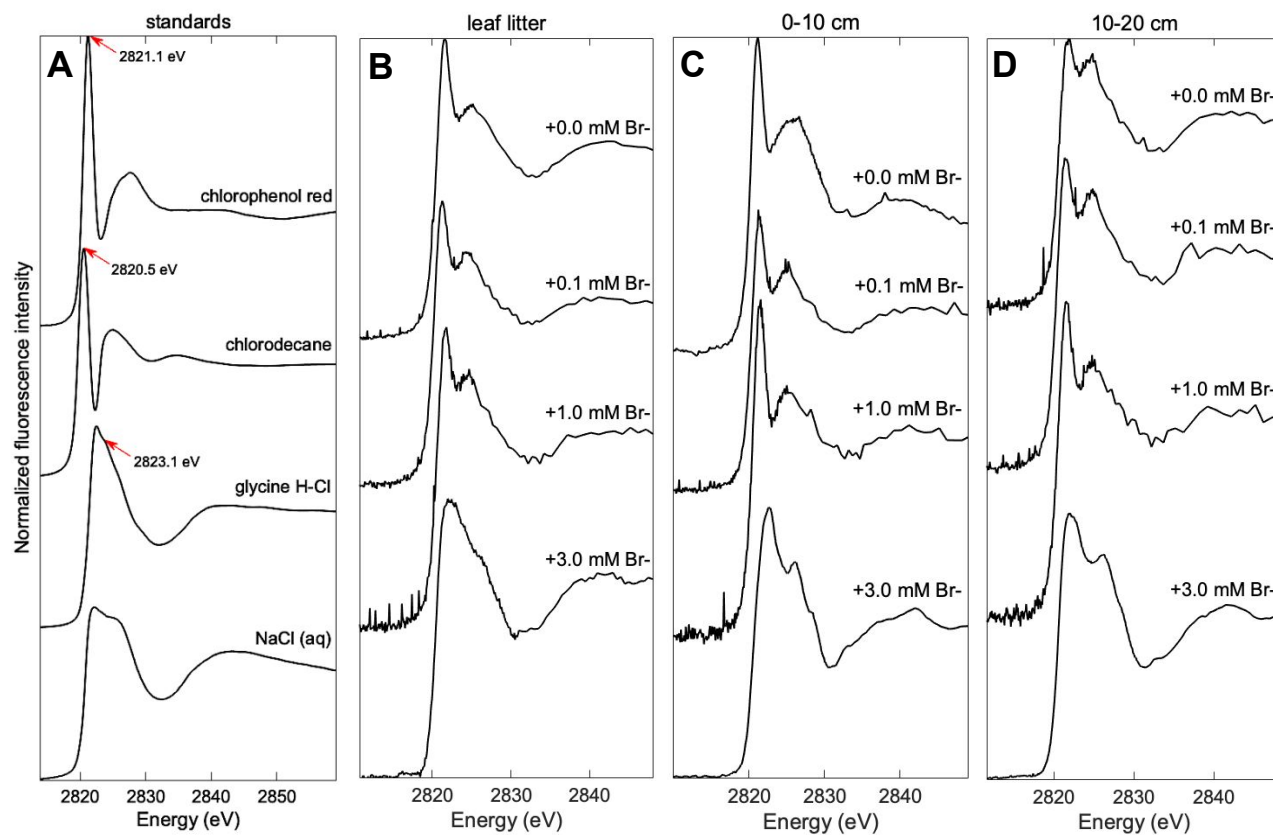
1
2
3 460 Energy, Office of Science, Office of Basic Energy Sciences under Contract No. DE-AC02-
4 76SF00515. This research used resources of the Advanced Photon Source, a U.S. Department of
5 461 Energy (DOE) Office of Science User Facility operated for the DOE Office of Science by Argonne
6 462 National Laboratory under Contract No. DE-AC02-06CH11357. We acknowledge the support of
7 463 GeoSoilEnviroCARS (Sector 13), which is supported by the National Science Foundation - Earth
8 464 Sciences (EAR-1128799), and the Department of Energy, Geosciences (DE-FG02-94ER14466).
9 465 This research used beamline 5-ID (SRX) of the National Synchrotron Light Source II, a U.S.
10 466 Department of Energy (DOE) Office of Science User Facility operated for the DOE Office of
11 467 Science by Brookhaven National Laboratory under Contract No. DE-SC0012704.
12
13
14
15
16
17
18
19
20
21
22
23
24
25

26 470 **References:**

- 27 471 (1) Myneni, S. C. B. Formation of Stable Chlorinated Hydrocarbons in Weathering Plant
28 472 Material. *Science* **2002**, *295* (5557), 1039–1041. <https://doi.org/10.1126/science.1067153>.
29 473 (2) Leri, A. C.; Marcus, M. A.; Myneni, S. C. B. X-Ray Spectromicroscopic Investigation of
30 474 Natural Organochlorine Distribution in Weathering Plant Material. *Geochim. Cosmochim.*
31 475 *Acta* **2007**, *71* (23), 5834–5846. <https://doi.org/10.1016/j.gca.2007.09.001>.
32 476 (3) Putschew, A.; Keppler, F.; Jekel, M. Differentiation of the Halogen Content of Peat
33 477 Samples Using Ion Chromatography after Combustion (TX/TOX-IC). *Anal. Bioanal.*
34 478 *Chem.* **2003**, *375* (6), 781–785. <https://doi.org/10.1007/s00216-003-1797-1>.
35 479 (4) Leri, A. C.; Hay, M. B.; Lanzirrotti, A.; Rao, W.; Myneni, S. C. B. Quantitative
36 480 Determination of Absolute Organohalogen Concentrations in Environmental Samples by X-
37 481 Ray Absorption Spectroscopy. *Anal. Chem.* **2006**, *78* (16), 5711–5718.
38 482 <https://doi.org/10.1021/ac060476m>.
39 483 (5) Biester, H.; Keppler, F.; Putschew, A.; Martinez-Cortizas, A.; Petri, M. Halogen Retention,
40 484 Organohalogens, and the Role of Organic Matter Decomposition on Halogen Enrichment in
41 485 Two Chilean Peat Bogs. *Environ. Sci. Technol.* **2004**, *38* (7), 1984–1991.
42 486 <https://doi.org/10.1021/es0348492>.
43 487 (6) Öberg, G.; Sandén, P. Retention of Chloride in Soil and Cycling of Organic Matter-Bound
44 488 Chlorine. *Hydrol. Process.* **2005**, *19* (11), 2123–2136. <https://doi.org/10.1002/hyp.5680>.
45 489 (7) Ortiz-Bermudez, P.; Srebotnik, E.; Hammel, K. E. Chlorination and Cleavage of Lignin
46 490 Structures by Fungal Chloroperoxidases. *Appl. Environ. Microbiol.* **2003**, *69* (8), 5015–
47 491 5018. <https://doi.org/10.1128/AEM.69.8.5015-5018.2003>.
48 492 (8) Ortiz-Bermudez, P.; Hirth, K. C.; Srebotnik, E.; Hammel, K. E. Chlorination of Lignin by
49 493 Ubiquitous Fungi Has a Likely Role in Global Organochlorine Production. *Proc. Natl.*
50 494 *Acad. Sci.* **2007**, *104* (10), 3895–3900. <https://doi.org/10.1073/pnas.0610074104>.
51
52
53
54
55
56
57
58
59
60

- 1
2
3 495 (9) Comba, P.; Kerscher, M.; Krause, T.; Schöler, H. F. Iron-Catalysed Oxidation and
4 496 Halogenation of Organic Matter in Nature. *Environ. Chem.* **2015**, *12* (4), 381.
5 497 <https://doi.org/10.1071/EN14240>.
6
7 498 (10) Singh, Z. Toxic Effects of Organochlorine Pesticides: A Review. *Am. J. Biosci.* **2016**, *4* (3),
8 499 11. <https://doi.org/10.11648/j.ajbio.s.2016040301.13>.
9 500 (11) Kutz, F. W.; Wood, P. H.; Bottimore, D. P. Organochlorine Pesticides and Polychlorinated
10 501 Biphenyls in Human Adipose Tissue*. In *Reviews of Environmental Contamination and*
11 502 *Toxicology*; Ware, G. W., Ed.; Reviews of Environmental Contamination and Toxicology;
12 503 Springer New York: New York, NY, 1991; pp 1–82. [https://doi.org/10.1007/978-1-4612-](https://doi.org/10.1007/978-1-4612-3080-9_1)
13 504 [3080-9_1](https://doi.org/10.1007/978-1-4612-3080-9_1).
14
15 505 (12) Jamil, D. K.; Shaik, A. P.; Mahboob, M.; Krishna, D. Effect of Organophosphorus and
16 506 Organochlorine Pesticides (Monochrotophos, Chlorpyrifos, Dimethoate, and Endosulfan)
17 507 on Human Lymphocytes In-Vitro. *Drug Chem. Toxicol.* **2005**, *27* (2), 133–144.
18 508 <https://doi.org/10.1081/DCT-120030725>.
19 509 (13) Molina, M. J.; Rowland, F. S. Stratospheric Sink for Chlorofluoromethanes: Chlorine
20 510 Atom-Catalysed Destruction of Ozone. *Nature* **1974**, *249* (5460), 810.
21 511 <https://doi.org/10.1038/249810a0>.
22
23 512 (14) Hossaini, R.; Chipperfield, M. P.; Feng, W.; Breider, T. J.; Atlas, E.; Montzka, S. A.;
24 513 Miller, B. R.; Moore, F.; Elkins, J. The Contribution of Natural and Anthropogenic Very
25 514 Short-Lived Species to Stratospheric Bromine. *Atmospheric Chem. Phys.* **2012**, *12* (1),
26 515 371–380. <https://doi.org/10.5194/acp-12-371-2012>.
27 516 (15) Joe-Wong, C.; Schlesinger, D. R.; Chow, A. T.; Myneni, S. C. B. Sea Level Rise Produces
28 517 Abundant Organobromines in Salt-Affected Coastal Wetlands. *Geochem. Perspect. Lett.*
29 518 **2019**, 31–35. <https://doi.org/10.7185/geochemlet.1911>.
30
31 519 (16) Hughes, Z. J.; FitzGerald, D. M.; Wilson, C. A.; Pennings, S. C.; Więski, K.; Mahadevan,
32 520 A. Rapid Headward Erosion of Marsh Creeks in Response to Relative Sea Level Rise.
33 521 *Geophys. Res. Lett.* **2009**, *36* (3). <https://doi.org/10.1029/2008GL036000>.
34 522 (17) Wang, J.-J.; Jiao, Y.; Rhew, R.; Chow, A. Haloform Formation in Coastal Wetlands along a
35 523 Salinity Gradient at South Carolina, United States. *Environ. Chem.* **2016**, *13*.
36 524 <https://doi.org/10.1071/EN15145>.
37
38 525 (18) National Weather Service - Climate Data
39 526 <https://w2.weather.gov/climate/getclimate.php?wfo=ilm> (accessed Feb 10, 2020).
40 527 (19) Morel, F. M. M.; Hering, J. G. *Principles and Applications of Aquatic Chemistry*, 1 edition.;
41 528 Wiley-Interscience: New York, 1993.
42 529 (20) Ravel, B.; Newville, M. ATHENA, ARTEMIS, HEPHAESTUS: Data Analysis for X-Ray
43 530 Absorption Spectroscopy Using IFEFFIT. *J. Synchrotron Radiat.* **2005**, *12* (4), 537–541.
44 531 <https://doi.org/10.1107/S0909049505012719>.
45
46 532 (21) Leri, A. C.; Myneni, S. C. B. Organochlorine Turnover in Forest Ecosystems: The Missing
47 533 Link in the Terrestrial Chlorine Cycle. *Glob. Biogeochem. Cycles* **2010**, *24* (4).
48 534 <https://doi.org/10.1029/2010GB003882>.
49 535 (22) MicroAnalysis Toolkit - XRF Imaging Processing Software [https://www.sams-](https://www.sams-xrays.com/smak)
50 536 [xrays.com/smak](https://www.sams-xrays.com/smak) (accessed Jan 1, 2019).
51 537 (23) Newville, M. Larch: An Analysis Package for XAFS and Related Spectroscopies. *J. Phys.*
52 538 *Conf. Ser.* **2013**, *430*, 012007. <https://doi.org/10.1088/1742-6596/430/1/012007>.
53
54
55
56
57
58
59
60

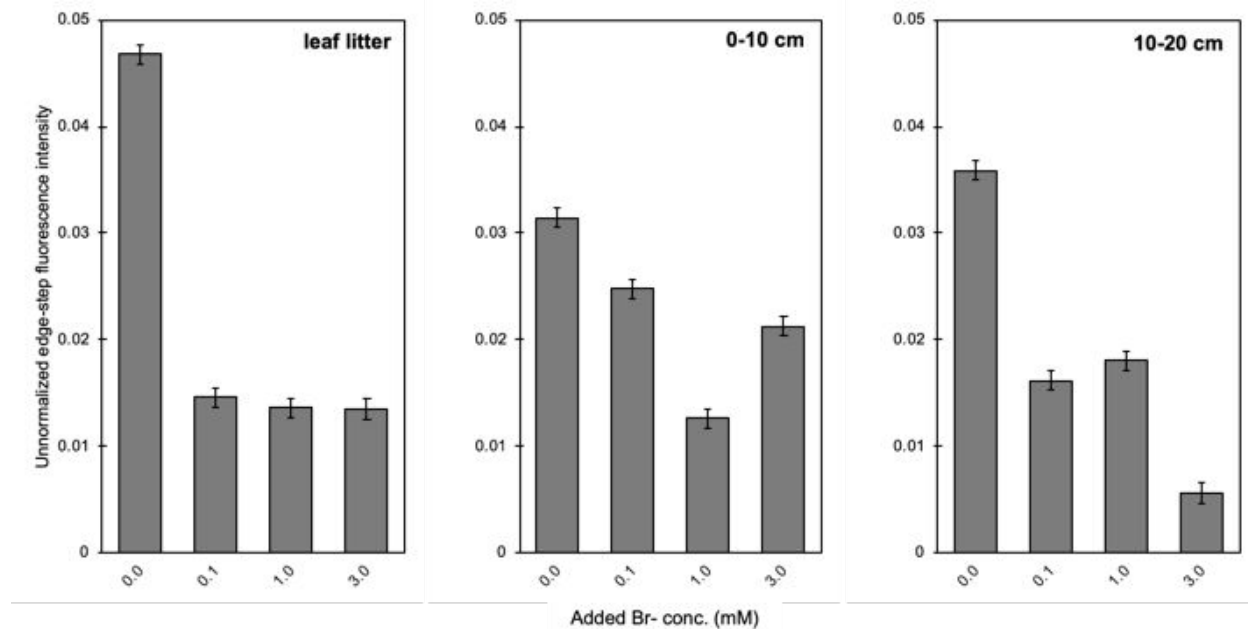
- 1
2
3 539 (24) Reina, R. G.; Leri, A. C.; Myneni, S. C. B. Cl K-Edge X-Ray Spectroscopic Investigation
4 540 of Enzymatic Formation of Organochlorines in Weathering Plant Material. *Environ. Sci.*
5 541 *Technol.* **2004**, *38* (3), 783–789. <https://doi.org/10.1021/es0347336>.
6
7 542 (25) Shokri-Kuehni, S. M. S.; Vetter, T.; Webb, C.; Shokri, N. New Insights into Saline Water
8 543 Evaporation from Porous Media: Complex Interaction between Evaporation Rates,
9 544 Precipitation, and Surface Temperature: Saline Water Evaporation From Sand. *Geophys.*
10 545 *Res. Lett.* **2017**, *44* (11), 5504–5510. <https://doi.org/10.1002/2017GL073337>.
11 546 (26) Shokri, N. Pore-Scale Dynamics of Salt Transport and Distribution in Drying Porous
12 547 Media. *Phys. Fluids* **2014**, *26* (1), 012106. <https://doi.org/10.1063/1.4861755>.
13 548 (27) Gribble, G. W. *Naturally Occurring Organohalogen Compounds - A Comprehensive*
14 549 *Update*; Springer Science & Business Media, 2009.
15
16 550 (28) Agarwal, V.; Miles, Z. D.; Winter, J. M.; Eustáquio, A. S.; El Gamal, A. A.; Moore, B. S.
17 551 Enzymatic Halogenation and Dehalogenation Reactions: Pervasive and Mechanistically
18 552 Diverse. *Chem. Rev.* **2017**, *117* (8), 5619–5674.
19 553 <https://doi.org/10.1021/acs.chemrev.6b00571>.
20 554 (29) Rhew, R. C.; Miller, B. R.; Weiss, R. F. Natural Methyl Bromide and Methyl Chloride
21 555 Emissions from Coastal Salt Marshes. *Nature* **2000**, *403* (6767), 292.
22 556 <https://doi.org/10.1038/35002043>.
23
24 557 (30) Jiao, Y.; Ruecker, A.; Deventer, M. J.; Chow, A. T.; Rhew, R. C. Halocarbon Emissions
25 558 from a Degraded Forested Wetland in Coastal South Carolina Impacted by Sea Level Rise.
26 559 *ACS Earth Space Chem.* **2018**, *2* (10), 955–967.
27 560 <https://doi.org/10.1021/acsearthspacechem.8b00044>.
28 561
29
30
31 562
32
33 563
34
35 564
36
37
38 565
39
40 566
41
42 567
43
44 568
45
46
47 569
48
49 570
50
51
52
53
54
55
56
57
58
59
60



571
572 Fig. 1) Normalized Cl XANES spectra of standards (A) and wetland samples (B-D). B: leaf litter, C: 0-
573 10 cm soil depth, and D: 10-20 cm soil depth. Spectra in panels B-D correspond to samples reacted with
574 increasing Br- concentration from top to bottom, and the topmost spectrum of 0.0 mM Br- indicates
575 control (the Br spectrum of this sample represents native Br in the sample). Arrows in panel A indicate
576 edge energies for Cl in different bonding environments, and these energies were used for Cl-speciation
577 maps presented in Fig. 3.

578

579



580

581 Fig. 2) In-situ estimation of Cl abundances in soils reacted with aqueous Br. The Cl abundance in these
582 wet samples was estimated directly using the unnormalized XANES spectral intensity of the edge step.

583

584

585

586

587

588

589

590

591

592

593

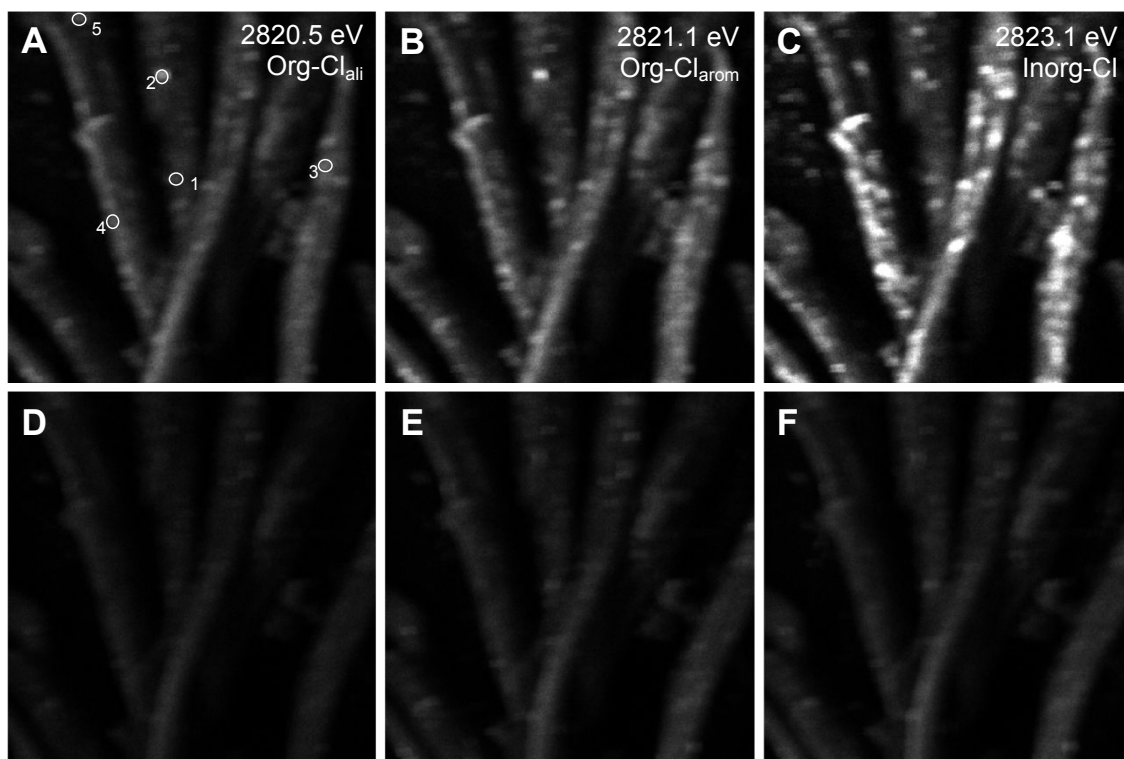
594

595

596

597

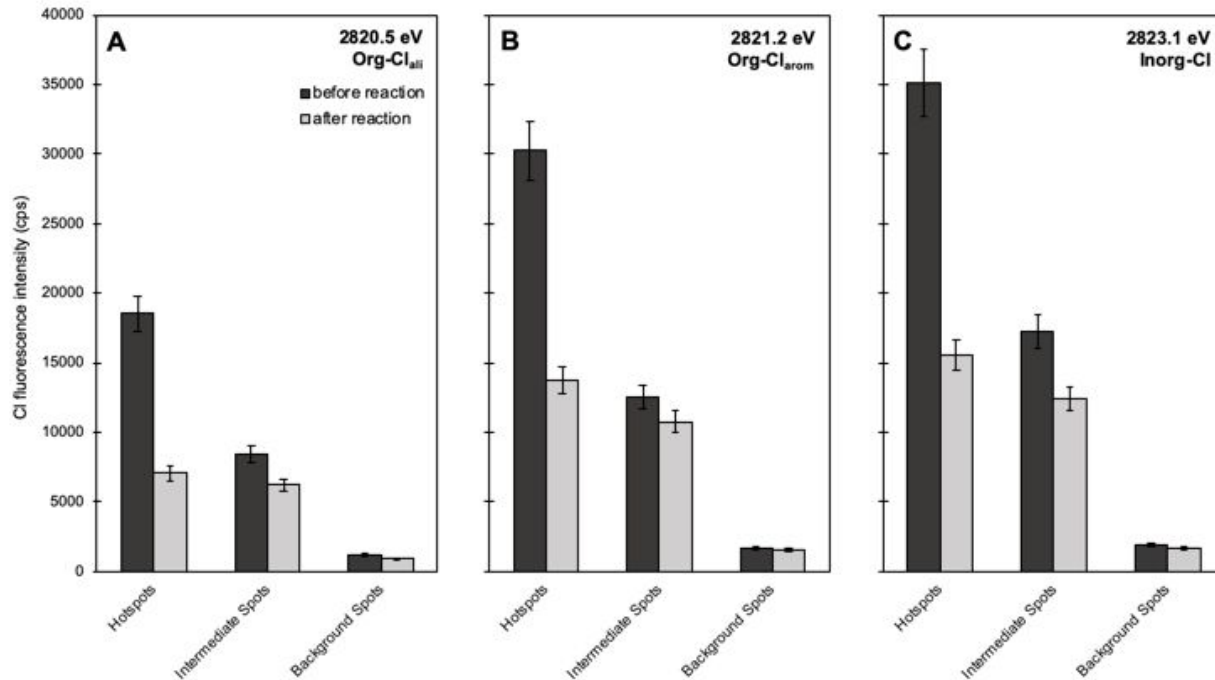
598



588

589 Fig. 3) Cl speciation of leaf litter before and after reaction with 0.1 mM Br. Maps A, B, and C show the
590 leaf before reaction with Br, and D, E, and F show the same after reaction with Br. Maps A and D were
591 collected at the aliphatic Org-Cl edge energy, 2820.5 eV. Maps B and E were collected at the aromatic
592 Org-Cl edge energy, 2821.1 eV. Maps C and F were done at the inorganic Cl edge energy, 2823.1 eV.
593 Spots 1-5, marked in map A, are locations where μ -XANES were collected both before and after reaction
594 with Br. These μ -XANES spectra are shown in Fig. S3.

595



596

597 Fig. 4) Changes in Cl abundance in different regions in leaf litter before and after reacting with 0.1 mM
598 Br. These data are derived from spectromicroscopy studies of leaf litter shown in Fig. 3. A: Org-Cl_{ali}, B:
599 Org-Cl_{arom}, and C: Inorg-Cl. The same spots were measured before and after reaction for comparison.
600 Hotspots and background spots are an average of 10 measured spots and intermediate spots indicate an
601 average of 5 measured spots in each map.

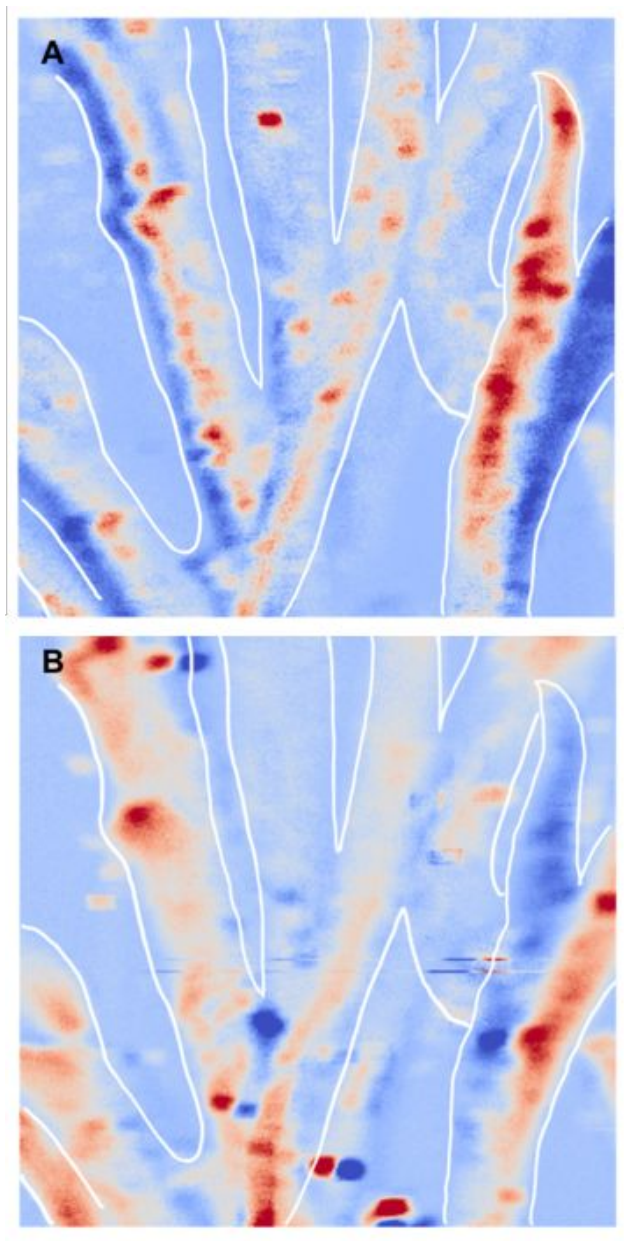
602

603

604

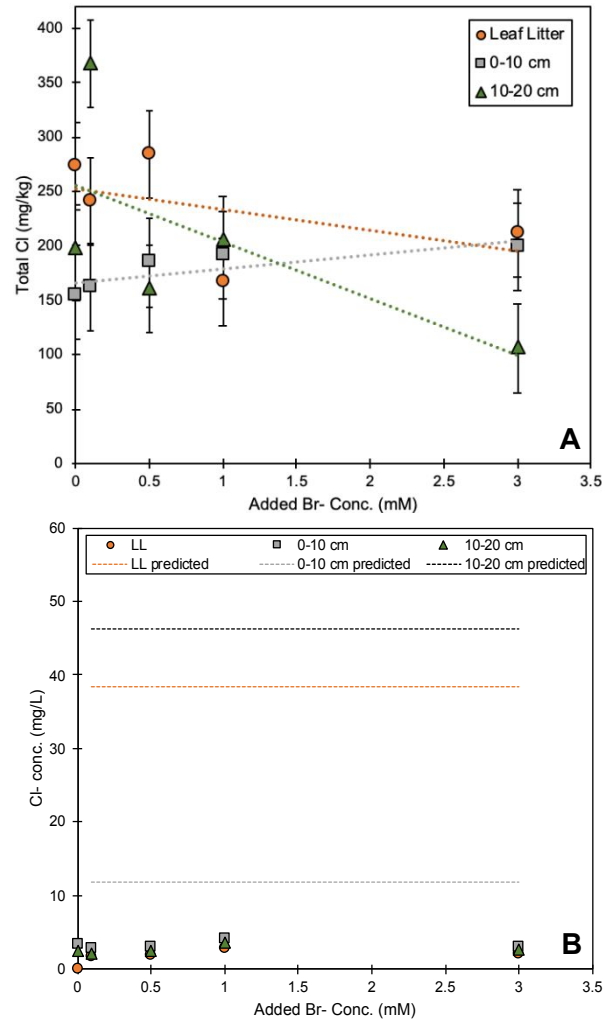
605

606



607
608 Fig. 5) Locations of bromination and org-Cl loss from leaf litter during exposure to aqueous Br⁻. White
609 outlines are used as a visual guide to indicate the outlines of the leaf branches. **A:** Fluorescence intensity
610 change of org-Cl before and after reaction with Br⁻ calculated by $\text{org-Cl}^{\text{before}} - \text{org-Cl}^{\text{after}}$. Red spots
611 indicate locations of highest org-Cl concentration prior to reaction with Br⁻. **B:** Fluorescence intensity
612 change of org-Br before and after reaction with Br⁻ calculated by $\text{org-Br}^{\text{after}} - \text{org-Br}^{\text{before}}$. Red spots
613 indicate locations of highest org-Br concentration following reaction with Br⁻.

614



615
 616 Fig. 6) **A**: Ex-situ XRF analysis of Cl in Br reacted, dried soils and leaf litter. Dashed lines indicate
 617 general trend lines for each soil depth. **B**: Aqueous phase analysis of Cl species by ion chromatography
 618 (IC). Br. Dashed lines indicate the predicted Cl⁻ concentration if all observed org-Cl loss is reduced to the
 619 inorg Cl⁻ form (70% for leaf litter, 38% for 0-10 cm, and 63% for 10-20 cm). Error is within 1%, error
 620 bars were too small to visualize on the graph.

621

622

623

624

625 **Table 1.** Solid phase Cl speciation in samples exposed to aqueous Br⁻. Speciation is from LCF of Cl-
 626 XANES spectra, and the Cl standards used are: chlorophenol red, chlorodecane, glycine H-Cl, and NaCl
 627 (aq) representing Cl bound to aromatic C, aliphatic-C, H-bonded Cl⁻, and hydrated inorganic Cl⁻,
 628 respectively (shown in Fig. 1A). Estimated fit error is ±3%.

Depth	Br ⁻ added (mM)	% Org-Cl _{ali}	% Org-Cl _{arom}	% Inorg-Cl H-bonded	% Inorg-Cl hydrated Cl ⁻
Leaf litter	0	11.2	39.0	49.8	0
	0.1	28.9	30.7	40.3	0
	1	10.6	31.6	57.7	0
	3	8.6	23.0	61.4	7.0
0-10 cm	0	28.1	29.4	0	42.5
	0.1	21.8	35.7	42.4	0
	1	10.6	47.5	41.9	0
	3	5.0	13.5	56.9	24.6
10-20 cm	0	13.6	21.8	52.6	12.0
	0.1	20.8	29.6	49.6	0
	1	12.8	37.8	49.5	0
	3	8.3	12.8	30.4	48.4

629

1
2
3
4
5
6
7
8
9
10
11
12
13
14
15
16
17
18
19
20
21
22
23
24
25
26
27
28
29
30
31
32
33
34
35
36
37
38
39
40
41
42
43
44
45
46
47
48
49
50
51
52
53
54
55
56
57
58
59
60

